ACCOUNTS of chemical research

Article

pubs.acs.org/accounts

Creation of Novel Solid-Solution Alloy Nanoparticles on the Basis of Density-of-States Engineering by Interelement Fusion

Hirokazu Kobayashi,[†,‡] Kohei Kusada,[†,‡] and Hiroshi Kitagawa*[,†,‡,§,∥]

[†]Division of Chemistry, Graduate School of Science, Kyoto University, Kitashirakawa-Oiwakecho, Sakyo-ku, Kyoto 606-8502, Japan
[‡]CREST, Japan Science and Technology Agency (JST), 7 Goban-cho, Chiyoda-ku, Tokyo 102-0076, Japan
[§]Institute for Integrated Cell-Material Sciences (iCeMS), Kyoto University, Yoshida, Sakyo-ku, Kyoto 606-8501, Japan
[∥]INAMORI Frontier Research Center, Kyushu University, Motooka 744, Nishi-ku, Fukuoka 819-0395, Japan

CONSPECTUS: Currently 118 known elements are represented in the periodic table. Of these 118 elements, only about 80 elements are stable, nonradioactive, and widely available for our society. From the viewpoint of the "elements strategy", we need to make full use of the 80 elements to bring out their latent ability and create innovative materials. Furthermore, there is a strong demand that the use of rare or toxic elements be reduced or replaced while their important properties are retained. Advanced science and technology could create higher-performance materials even while replacing or reducing minor or harmful elements through the combination of more abundant elements.

The properties of elements are correlated directly with their electronic states. In a solid, the magnitude of the density of states (DOS) at the Fermi level affects the physical and chemical properties. In the present age, more attention has been paid to improving the properties of materials by means of alloying elements. In particular, the solid-solution-type alloy is advantageous because the properties can be continuously controlled by tuning the compositions and/or combinations of the constituent elements. However, the majority of bulk alloys are of the phase-separated type under ambient conditions, where constituent elements are immiscible with each other. To overcome the challenge of the bulk-phase metallurgical aspects, we have focused on the nanosize effect and developed methods involving "nonequilibrium synthesis" or "a process of hydrogen absorption/desorption". We propose a new concept of "density-of-states engineering" for the design of materials having the most desirable and suitable properties by means of "interelement fusion".

In this Account, we describe novel solid-solution alloys of Pd−Pt, Ag−Rh, and Pd−Ru systems in which the constituent elements are immiscible in the bulk state. The homogeneous solid-solution alloys of Pd and Pt were created from Pd core/Pt shell nanoparticles using a hydrogen absorption/desorption process as a trigger. Several atom percent replacements of Pd with Pt atoms resulted in a significantly enhanced hydrogen absorption capacity compared with Pd nanoparticles. Ag_xRh_{1-x} and Pd_xRu_{1-x} solid-solution alloy nanoparticles were also developed by nonequilibrium synthesis based on a polyol method. The Ag_xRh_{1-x} nanoparticles demonstrated hydrogen storage properties, although pure metal nanoparticles of each constituent element do not adsorb hydrogen. Ag_xRh_{1-x} is therefore considered to possess a similar electronic structure to Pd as a synthetic pseudo-palladium. The Pd_xRu_{1-x} nanoparticles showed enhanced catalytic activity for CO oxidation, with the highest catalytic activity found using the equimolar $Pd_{0.5}Ru_{0.5}$ nanoparticles. The catalytic activity of the $Pd_{0.5}Ru_{0.5}$ nanoparticles exceeds that of the widely used and best-performing Ru catalysts for CO oxidation and is also higher than that of neighboring Rh on the periodic table. Our present work provides a guiding principle for the design of a suitable DOS shape according to the intended physical and/or chemical properties and a method for the development of novel solid-solution alloys.

1. INTRODUCTION

Currently 118 known elements are represented in the periodic table. Of these 118 elements, only about 80 elements are stable, nonradioactive, and widely available for our society. From the viewpoint of the "elements strategy",[1] we need to make full use of the 80 elements to bring out their latent ability and create innovative materials. Society strongly demands that rare or toxic elements should be reduced or replaced while their properties are retained. However, advanced science and technology could create higher-performance materials even while replacing or reducing minor or harmful elements through the combination of more abundant elements.

The chemical and physical properties of the elements are correlated directly with their electronic states. According to frontier orbital theory, in a molecule the highest occupied molecular orbital (HOMO) and lowest unoccupied molecular orbital (LUMO) are crucial in governing chemical reactions.[2] On the other hand, in a solid the magnitude of the density of states (DOS) at the Fermi level (E_F) affects physical properties such as transport, magnetic, optical, electronic heat capacity, and thermal properties, etc.[3] For example, the group-10

Received: November 14, 2014
Published: May 20, 2015

DOI: 10.1021/ar500413e
Acc. Chem. Res. 2015, 48, 1551−1559

element palladium exhibits strong paramagnetism depending on the temperature because of the high DOS at E_F and is well-known as a nearly ferromagnetic metal.[4] With respect to the catalytic properties of Pd, the unoccupied and occupied high DOS of the 4d band around E_F can act as an effective electron acceptor and donor to many reactants, providing good catalytic activities in both oxidation and reduction reactions, respectively.[5−7] On the other hand, the group-11 metal gold is a good electronic conductor as a result of the broad 6s band at E_F. However, the inactivity of Au in many catalytic reactions is considered to originate from a low DOS at E_F.

Alloys are ubiquitous in human history, with tools developed from alloys defining much of our history from early civilization. They have been at the forefront of technological advancement in our history, as alloying allows us to improve the mechanical properties of useful metals. In the present age, more attention has been paid to improving physical properties by alloying. Thus, alloying is a useful method for improving not only structural but also physical properties. In general, there are two types of alloy, namely, phase-separated and solid-solution types. The former is not suitable for continuous control of chemical and physical properties, and the latter is more favorable because the constituent elements of a solid solution are randomly and homogeneously distributed. However, the majority of the bulk alloys are phase-separated under ambient conditions, where the constituent elements are immiscible with each other.[8] We face a serious challenge in developing a variety of alloy materials because we cannot freely choose the combination of elements.

To overcome the challenge of the bulk-phase metallurgical aspects, we have focused on the nanosize effect. Metal nanoparticles are known to show different chemical and physical properties from bulk metals because of their high surface-to-volume ratios and the quantum size effect.[9,10] In particular, nanosizing provides different phase behavior from the bulk, such as melting point depression[11,12] or spontaneous alloying[13,14]. For example, the melting point of Au (1610 °C) decreases with a decrease in the mean diameter, and the melting temperature of sub-3 nm nanoparticles is ∼300 K lower than that of bulk Au.[11] In addition, in Au−Ag and Au−Cu systems, where the solid solution is the thermodynamically stable phase, spontaneous alloying was observed at room temperature.[13,14] Very recently, nonequilibrium synthetic techniques have allowed us to obtain unknown materials with a thermodynamically unstable/metastable phase. For example, novel face-centered-cubic (fcc) Ru was discovered in the nanometer region, while hexagonal close-packed (hcp) is the only phase in bulk Ru.[15] Thus, a decrease in size alters the thermodynamic properties, causing deviations from the phase diagram of the bulk metal. Nanosizing is considered to be a powerful tool in creating novel solid-solution alloys that do not exist in equilibrium in the bulk state.

Here we propose a new concept of "DOS engineering" for the design of materials with the most desirable and suitable properties by means of "interelement fusion". For example, in CO adsorption on the transition-metal surface, the adsorption property is generally explained in terms of two bonding forms:[16] CO σ donation to the unoccupied metal e_g orbitals and metal π back-donation from the occupied metal t_{2g} orbitals to CO. Therefore, to create an efficient CO adsorbent, we should design a material with a high DOS at the unoccupied e_g and occupied t_{2g} orbitals. For high-performance catalysts in oxidation and reduction reactions, a high DOS of unoccupied and occupied states, respectively, around E_F is required. From this point of view, the reason Pd and Pt show high catalytic activities for both oxidation and reduction reactions originates from the higher DOS of both occupied and unoccupied orbitals compared with other metals, such as Ag or Au (Figure 1). In addition, E_F of Pd or Pt is located at the highest DOS composed mainly of d bands, which also contributes to the efficient catalytic properties.

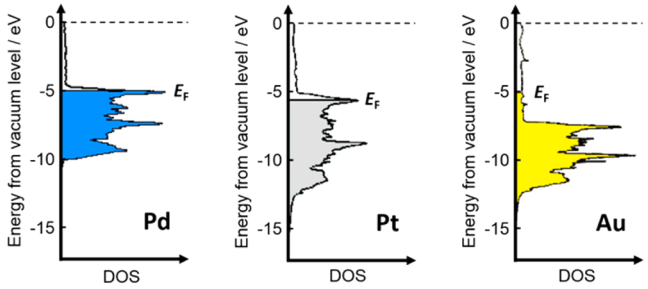

Figure 1. Band structures of Pd, Pt, and Au around the Fermi level.[17]

To date, a d-band theory has been proposed for catalytic design, which is based on tuning of the location of the d-band center.[18,19] Hence, the design of not only the location of the d-band center but also the suitable DOS shape according to the intended chemical and physical properties is very important; this is DOS engineering. To manipulate the shape of the DOS freely, we need to use not only d-group elements but also every available element, including the s, p, and f groups by means of interelement fusion (Figure 2).

In this Account, we introduce three novel solid-solution alloys created by approaches involving nonequilibrium synthesis or a process of hydrogen absorption/desorption. The PdPt and AgRh solid-solution alloys exhibit enhanced hydrogen storage properties, and PdRu solid-solution alloys showed enhancement of the catalytic properties for CO oxidation.

2. PDPT SOLID-SOLUTION FORMATION BY A PROCESS OF HYDROGEN ABSORPTION/DESORPTION: THE ENHANCED HYDROGEN STORAGE CAPACITY OF PD

Pd and Pt are catalysts in many important industrial applications, including fuel-cell technology, organic synthesis, and automobile catalytic conversion.[5−7,20−22] These applications require nanosized Pd and Pt, which have high surface-to-volume ratios and unique electronic states that enhance their chemical and physical properties compared with those of the bulk. Certain types of nanostructured materials, such as core/shell or dendritic structures, can be obtained as nanoparticles but not as bulk phases.[23−25] In contrast, there are few reports regarding the structure of solid-solution alloy nanoparticles, where there is a homogeneous mixture of Pd and Pt at the atomic level.[26] The scarcity of reports regarding nanostructured homogeneous Pd/Pt alloys originates from the fact that Pd and Pt intrinsically segregate and form a domain structure.[27]In this section, we demonstrate the formation of a novel solid-solution alloy where Pd and Pt are mixed at the atomic level via a process of hydrogen absorption/desorption (PHAD) as a trigger for Pd core/Pt shell nanoparticles (Figure 3).[28]

Pd/Pt core/shell nanoparticles consisting of a 6.1 nm Pd core and a 1.1 nm Pt shell were used.[28] Inductively coupled plasma mass spectrometry (ICP-MS) showed that 21 atom % Pt was included in the Pd/Pt nanoparticles. Figure 4 shows the

DOI: 10.1021/ar500413e
Acc. Chem. Res. 2015, 48, 1551−1559

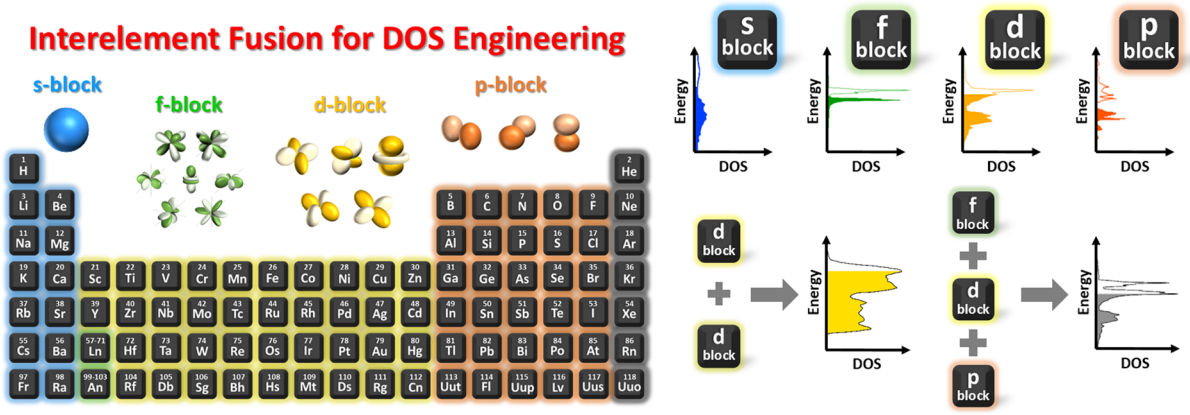

Figure 2. "Interelement fusion" strategy for innovative functional materials based on "DOS Engineering".

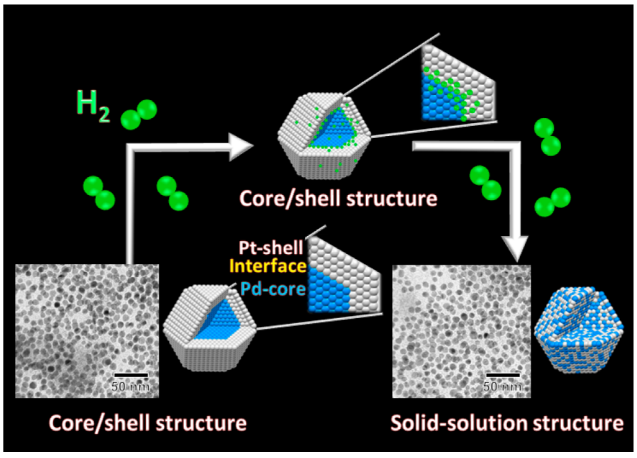

Figure 3. Structural change from the initial Pd core/Pt shell bimetallic nanoparticles into a PdPt solid solution by PHAD at 100 °C. TEM images show that aggregation between particles does not occur and that the particle size is maintained before and after the PHAD. Reprinted from ref 28. Copyright 2010 American Chemical Society.

in situ powder X-ray diffraction (XRD) patterns of the Pd/Pt core/shell nanoparticles during the PHAD at 100 °C. Under vacuum (0 kPa), the XRD pattern of the Pd/Pt core/shell nanoparticles consisted of two kinds of fcc patterns, and the diffraction peaks from the Pt shell were observed at the higher-angle side.[28,29] During the PHAD at 100 °C, the diffraction peaks of the Pd/Pt core/shell nanoparticles did not change, even though hydrogen absorption properties were observed. In contrast, during hydrogen desorption, the diffraction patterns from the Pd core and Pt shell portions disappeared, and a single fcc lattice pattern emerged as the hydrogen pressure was decreased. The lattice constants for the core and shell portions were determined separately by Le Bail pattern-fitting analysis (Figure 4c,d). During the hydrogen absorption process, the lattice constants in the Pd core and Pt shell remained unchanged between 0 and 101.3 kPa, indicating that the core/shell structure of the bimetallic nanoparticles was maintained. In contrast, during desorption, the lattice constant of the shell portion hardly changed, while that of the core portion became smaller with decreasing hydrogen pressure, and the overlap patterns coalesced into a single fcc lattice at 0 kPa. This result strongly suggests that the core/shell structure changes to a solid-solution structure with a single fcc lattice following PHAD treatment at 100 °C. High-resolution transmission electron microscopy (TEM) and nanospot energy-dispersive X-ray spectroscopy (EDX) demonstrated that the resulting PdPt nanoparticles formed a solid-solution alloy in which Pd and Pt were homogeneously mixed at the atomic level.[28]

The hydrogen absorption properties of metal nanoparticles are strongly correlated with their structure and the electronic state.[30−36] In order to investigate the hydrogen absorption properties of the novel PdPt solid-solution nanoparticles with varying alloy compositions obtained from the precursor core/shell nanoparticles via PHAD, we measured their hydrogen pressure−composition (PC) isotherms at 30 °C (Figure 5). Bulk Pt shows no ability to absorb hydrogen,[37] but when 8 atom % Pd was replaced with Pt in the nanoparticles, the amount of hydrogen absorption increased. A further increase in the percentage of Pt atoms resulted in a decrease in the hydrogen concentration, and the amount of absorbed hydrogen for the $Pd_{0.50}Pt_{0.50}$ solid-solution nanoparticles became smaller than that for Pd nanoparticles. These results demonstrated that the hydrogen storage capabilities of PdPt solid-solution nanoparticles can be controlled by changing the alloy composition on the basis of band filling of the PdPt solid-solution alloys. This discovery of a homogeneous solid-solution alloy of Pd and Pt will contribute substantially to catalysis and other material fields. Moreover, the PHAD method may enable us to design and construct novel alloys that have not been obtained to date as solid solutions.

3. SYNTHETIC PSEUDO-PD: AGRH SOLID-SOLUTION NANOPARTICLES EXHIBITING HYDROGEN STORAGE CAPABILITIES

Rh, Pd, and Ag are neighboring 4d transition metals with fcc structures, and all are used as efficient catalysts for a variety of important chemical reactions.[38−40] In light of the band-filling effect of the III−V compound semiconductors,[41] we expected that the $Ag_{0.5}Rh_{0.5}$ solid-solution alloy would possess an electronic structure and chemical/physical properties similar to those of Pd, since Rh and Ag are located on either side of Pd in the periodic table. For instance, Pd is well-known to exhibit a high hydrogen storage capability, which is related to its electronic structure;[42,43] if the hybridization of d orbitals and the band-filling effect can occur with AgRh solid-solution alloys, then $Ag_{0.5}Rh_{0.5}$ would also be expected to absorb hydrogen like Pd. A problem arises, however, because the Ag−Rh system is immiscible even above the melting temperature of Rh (1964 °C), that is, Rh and Ag (like oil and water) cannot mix at the

DOI: 10.1021/ar500413e
Acc. Chem. Res. 2015, 48, 1551−1559

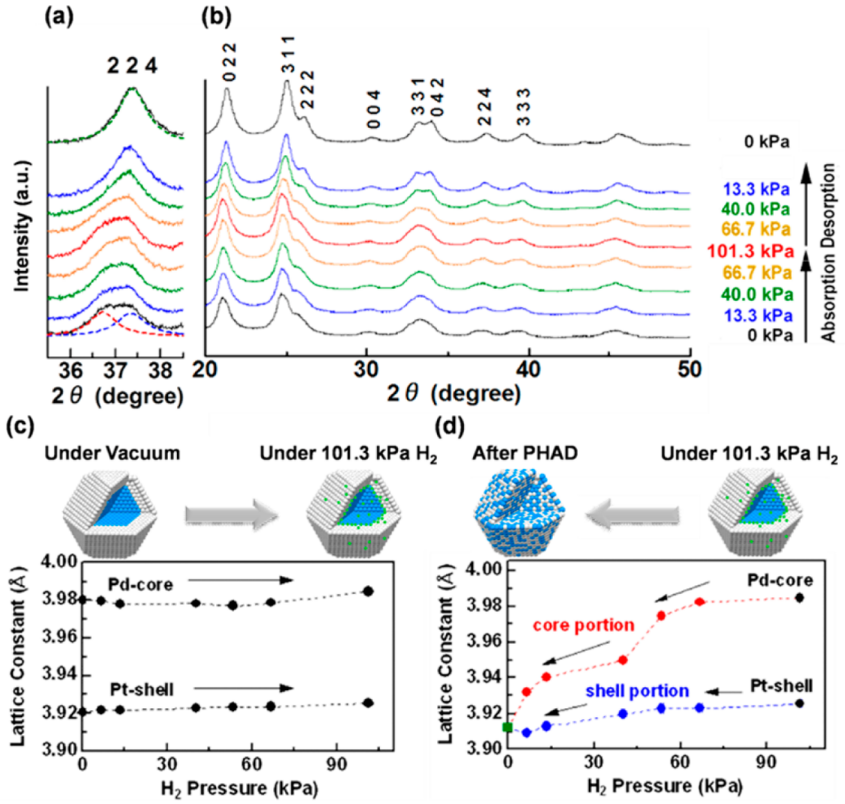

Figure 4. (a, b) In-situ powder XRD patterns of Pd/Pt nanoparticles upon PHAD at 100 °C. (c, d) Lattice constants estimated by Le Bail fitting to the diffraction patterns measured during the (c) hydrogen absorption and (d) desorption processes. (Pd core and Pt shell, black circles; core portion, red circles; shell portion, blue circles; PdPt solid solution, green square.) Reprinted from ref 28. Copyright 2010 American Chemical Society.

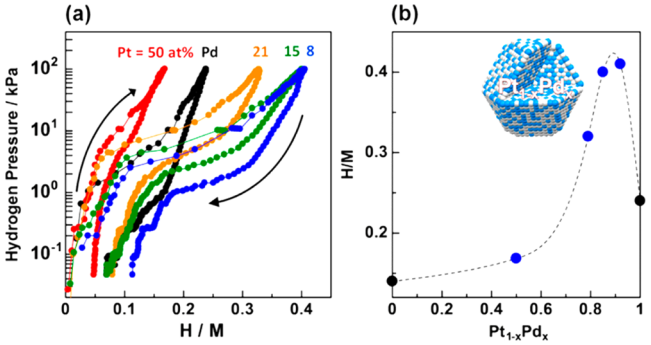

Figure 5. (a) PC isotherms of Pd, $Pd_{0.92}Pt_{0.08}$, $Pd_{0.85}Pt_{0.15}$, $Pd_{0.79}Pt_{0.21}$, and $Pd_{0.50}Pt_{0.50}$ solid-solution nanoparticles at 30 °C. The metal compositions of the PdPt nanoparticles were estimated by ICP-MS. Isotherms were measured according to the direction of the arrows. H/M shows the hydrogen-to-metal atomic ratio. (b) Dependence of H/M on the PdPt solid-solution alloy composition at 101.3 kPa. Reprinted from ref 28. Copyright 2010 American Chemical Society.

atomic level.[44] For this reason, solid-solution alloys of Ag and Rh had not previously been obtained, and the structure and properties of the alloys had not been investigated.

To obtain the AgRh solid-solution alloy nanoparticles, we adopted a modified polyol method. In our original method, the point of synthesis to obtain a solid-solution phase was to simultaneously reduce the both metal ions to metals. Hence, we added the metal precursors slowly to a fully heated ethylene glycol (EG) solution (Figure 6). Mixing both Ag^+ and Rh^{3+} ions with the EG solution prior to heating has a marked impact on the rates of reduction of Ag and Rh ions because Ag^+ is more easily reduced than Rh^{3+}, and as a result, Ag and Rh nanoparticles form as a phase-segregated mixture. To avoid phase segregation, we modified the synthesis by slowly adding the solution containing Rh^{3+} and Ag^+ to hot EG at 170 °C. The heated EG solution rapidly turned black, indicating that the Ag^+ and Rh^{3+} ions were rapidly reduced, so the difference in the rates of reduction could be considered negligible. This rapid simultaneous reduction of Ag^+ and Rh^{3+} precursors in hot EG allowed the synthesis of AgRh solid-solution nanoparticles.[45]

The solid-solution structure of AgRh nanoparticles was investigated using XRD, X-ray photoelectron spectroscopy (XPS), and scanning TEM (STEM)−EDX techniques. The Ag_xRh_{1-x} nanoparticles adopted a single fcc structure over the whole composition range, and the lattice parameter decreased continuously with increasing Rh content. The STEM−EDX maps show visual evidence of alloying (Figure 7).

Furthermore, the prepared Ag_xRh_{1-x} nanoparticles showed hydrogen storage properties. Although the amount of hydrogen absorption of $Ag_{0.5}Rh_{0.5}$ was less than that of Pd nanoparticles, the $Ag_{0.5}Rh_{0.5}$ alloy, which was expected to have a similar electronic structure to Pd, exhibited the largest amount of hydrogen absorption of the alloy system.[45]

The electronic structure of $Ag_{0.5}Rh_{0.5}$ nanoparticles was investigated using a combination of hard XPS (HAXPES) experiments and first-principles calculations.[46] Ag, Rh, and AgRh nanoparticles with similar sizes were used for the HAXPES experiments. In the core-level XPS spectrum of AgRh solid-solution nanoparticles, signals originating from Rh or Ag oxide were not observable.[45,46] The valence band (VB) HAXPES spectrum and calculated results for the $Ag_{0.5}Rh_{0.5}$ nanoparticles did not correspond to a simple linear

DOI: 10.1021/ar500413e
Acc. Chem. Res. 2015, 48, 1551−1559

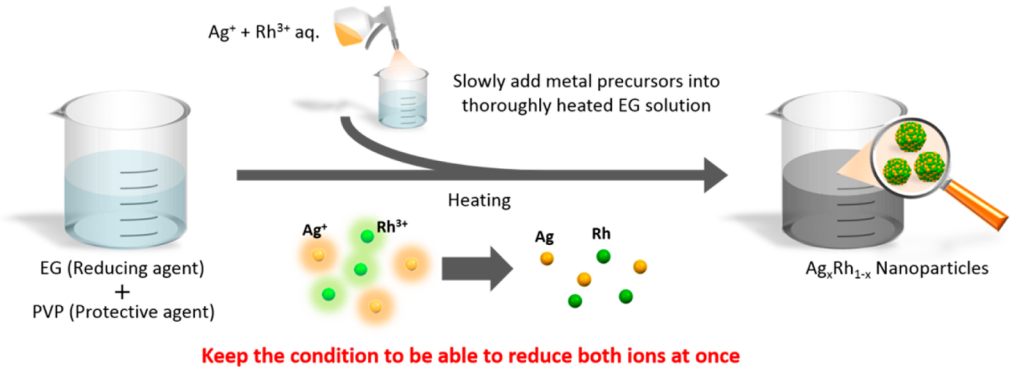

Figure 6. Schematic illustration of the synthesis of Ag_xRh_{1-x} nanoparticles.

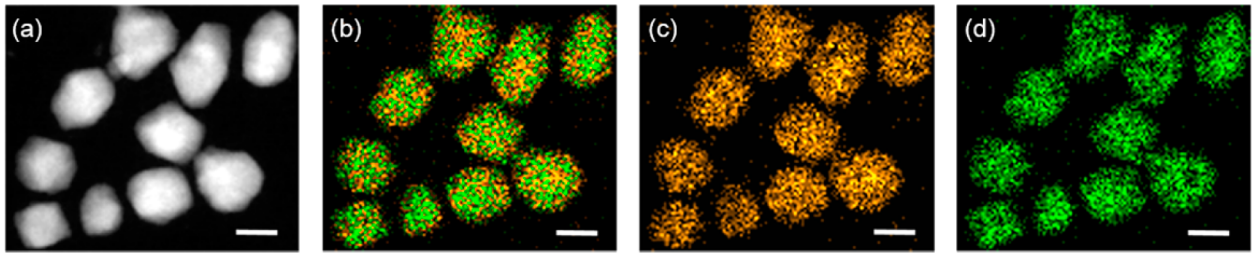

Figure 7. (a) High-angle annular dark-field STEM image of a group of prepared $Ag_{0.5}Rh_{0.5}$ nanoparticles. (b) Overlay image of the EDX maps shown in (c) and (d) (green, Rh; orange, Ag). (c) Ag and (d) Rh L-shell STEM−EDX maps. The scale bars correspond to 10 nm. Reprinted from ref 45. Copyright 2010 American Chemical Society.

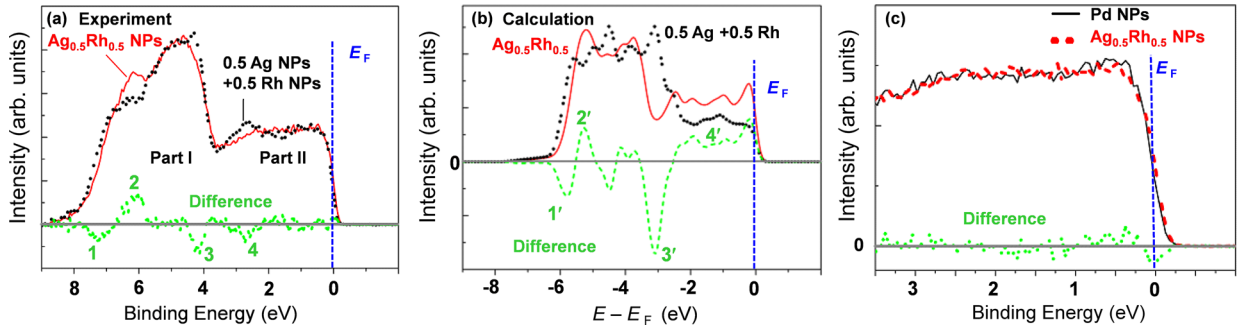

Figure 8. (a) VB HAXPES spectra and (b) calculated spectra corresponding to $Ag_{0.5}Rh_{0.5}$ (red) and the linear combination of the Ag and Rh spectra (0.5 Ag + 0.5 Rh, black). The difference spectrum (green) indicates the extent to which the spectrum of the alloy deviates from the linear combination. (c) VB HAXPES spectra of $Ag_{0.5}Rh_{0.5}$ alloy nanoparticles (enlarged, red) and Pd nanoparticles (black) in the E_b range of 0−3.5 eV. Reprinted with permission from ref 46. Copyright 2014 American Institute of Physics.

combination of the spectra for pure Ag and Rh nanoparticles (Figure 8a,b). The differences between the spectrum of the alloy nanoparticles and the linear summation of the Rh and Ag spectra indicate that hybridization of the orbitals occurred in the AgRh alloy nanoparticles.

As the electronic structure of the VB near the Fermi edge is more important for catalysts, the VB structures of the $Ag_{0.5}Rh_{0.5}$ alloy and Pd nanoparticles were compared in the binding energy (E_b) range of 0−3.5 eV (Figure 8c). The VB structures of the $Ag_{0.5}Rh_{0.5}$ alloy and Pd nanoparticles are very similar over this E_b range. The remarkable similarity provides the hydrogen capacity of the AgRh solid-solution alloy. The corresponding intensity of the $Ag_{0.5}Rh_{0.5}$ alloy nanoparticles was found to be about half that of the Pd nanoparticles in the energy range of interest.[46] This result was surprisingly accurate and quantitatively corresponded to the experimental result that the total amount of absorbed hydrogen of $Ag_{0.5}Rh_{0.5}$ alloy nanoparticles was about half of that of Pd nanoparticles.[45] These findings provide a guideline for the design and development of solid-solution alloys with interesting properties on the basis of DOS engineering.

4. SYNTHETIC PSEUDO-RH: PDRU SOLID-SOLUTION NANOPARTICLES HAVING ENHANCED CO OXIDIZING ABILITY

Ru, Rh, and Pd are neighboring 4d transition metals that are located in order of increasing atomic number in the periodic table, and in the bulk state Pd and Ru cannot form a solid-solution alloy over the whole metal composition range until both metals are liquid.[47] Therefore, PdRu solid-solution alloys cannot be easily obtained. We reported the first example of the synthesis of solid-solution alloy nanoparticles of Pd and Ru, the elements neighboring Rh, throughout the whole range of metal compositions using a chemical reduction method.

Rh and Ru are used as valuable catalysts for many important reactions, such as the reduction of NO_x and the oxidation of

DOI: 10.1021/ar500413e
Acc. Chem. Res. 2015, 48, 1551−1559

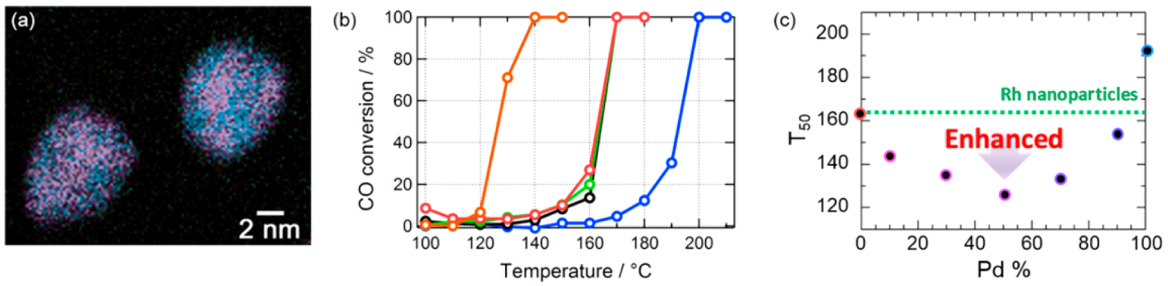

Figure 9. (a) Overlay image of the EDX maps of Pd and Ru for $Pd_{0.5}Ru_{0.5}$ nanoparticles. (b) Temperature dependence of the CO conversion by Ru (red), Rh (green), Pd (blue), $Pd_{0.5}Ru_{0.5}$ solid solution (orange), and Ru + Pd mixture (black) nanoparticles supported on γ-Al_2O_3. (c) Metal-composition dependence of T_{50} (in °C). Reprinted from ref 60. Copyright 2014 American Chemical Society.

CO.[48−51] Recently, because of the growing importance of CO removal from fuel-cell systems or car exhaust, many researchers have extensively developed CO oxidation catalysts.[52] Pd is also widely used as an efficient catalyst for exhaust gas purification and for polymer electrolyte fuel cell electrodes.[53,54] However, the Pd catalyst is easily poisoned by CO, which blocks surface binding sites and decreases the catalytic activity,[55] and it is therefore necessary to remove CO molecules from the system to optimize the efficiency. Furthermore, Ru has received much attention recently because it is a useful catalyst for the steam-reforming reaction of methane.[56,57] Methane is a main component of shale gas, and the share of synthesis gas obtained from the steam-reforming of shale gas has been growing. Because alloying with other elements often enhances the catalytic properties of these platinum-group metals,[58,59] the PdRu solid-solution alloy is expected to be a highly active catalyst for many applications.

On the basis of the results from the Ag−Rh system, the $Pd_{0.5}Ru_{0.5}$ alloy was also anticipated to have an electronic structure similar to that of Rh because Pd and Ru are located on either side of Rh in the periodic table. Although Rh is a very attractive element exhibiting highly effective catalytic activity, it is extremely expensive because of its scarcity. Pd and Ru are considerably cheaper than Rh, and thus, a PdRu alloy which mimics or improves on the properties of Rh is an important target in terms of the "elements strategy".[1]

Pd_xRu_{1-x} nanoparticles were obtained using a similar synthetic method as for the Ag_xRh_{1-x} nanoparticle synthesis. The solid-solution structure of Pd and Ru was confirmed using TEM, XRD, XPS, and STEM−EDX measurements.[60] The sizes of the Pd_xRu_{1-x} nanoparticles were similar, and the STEM−EDX maps showed visual evidence of the solid-solution structure (Figure 9a). The compositional line profiles of Ru and Pd on a $Pd_{0.5}Ru_{0.5}$ nanoparticle indicated that Pd and Ru atoms were dispersed homogeneously throughout the whole particle. With increasing Pd metal composition, the structure of the Pd_xRu_{1-x} nanoparticles changed from the Ru hcp lattice to the Pd fcc lattice. From the Rietveld refinement of the XRD patterns, the structures of Pd_xRu_{1-x} nanoparticles ($0.3 \leq x \leq 0.7$) included both hcp and fcc structures.[60] However, the metal ratios of Pd and Ru in the coexisting hcp and fcc structures were approximately same and were consistent with the average composition obtained from the EDX data. In addition, the lattice constants of both structures followed Vegard's rule. These results clearly showed that Pd and Ru were mixed at the atomic level over the whole metal composition range.[60]

The Pd_xRu_{1-x} solid-solution nanoparticles show higher catalytic activity for CO oxidation than Ru or Pd nanoparticles. Figure 9b presents a comparison of the CO oxidation results for 1 wt % γ-Al_2O_3-supported Pd_xRu_{1-x}, Rh, and a physical mixture of Ru and Pd nanoparticles. The temperatures for 50% conversion of CO to CO_2 (T_{50}) for $Pd_{0.5}Ru_{0.5}$, Rh, Ru, and Pd catalysts were approximately 125, 165, 165, and 195 °C, respectively. These results clearly show that the $Pd_{0.5}Ru_{0.5}$ nanoparticles exhibited higher activity for CO oxidation than other catalysts. While Ru was the most efficient CO oxidation catalyst, $Pd_{0.5}Ru_{0.5}$ converted CO to CO_2 at a temperature 30−40 K lower than that for Ru. Furthermore, $Pd_{0.5}Ru_{0.5}$ showed a lower conversion temperature than Rh, which is the most expensive precious metal, indicating that $Pd_{0.5}Ru_{0.5}$ nanoparticles are a more effective catalyst than Rh for the CO oxidation reaction. On the other hand, the physical mixture of Ru and Pd nanoparticles showed completely different catalytic properties from PdRu alloy nanoparticles, exhibiting almost the same activity as that of Ru nanoparticles because the Ru nanoparticles have higher activity than Pd nanoparticles and are dominant for this reaction. These results further confirm that interelement fusion strategy is a viable method for creating novel nanomaterials with enhanced properties while potentially offering further advantages such as reduced cost. The greatly enhanced catalytic ability of the PdRu alloy, like the hydrogen absorption properties of the AgRh alloys, is considered to result from the novel electronic structure arising from the formation of the solid-solution alloy of Pd and Ru.

Figure 9c shows the metal-composition dependence of the CO conversion in Pd_xRu_{1-x} nanoparticles supported on γ-Al_2O_3. The catalytic activities of all of the alloy nanoparticles are higher than those of pure Pd or Ru nanoparticles, and the activity is maximized at the $Pd_{0.5}Ru_{0.5}$ composition. The oxidation state of Ru has been reported to affect the catalytic activity of CO oxidation,[61] but the inverse-volcano-type behavior of T_{50} for Pd_xRu_{1-x} nanoparticles suggests that the oxidation states of Ru are not the dominant factor for CO oxidation activity in this system.

There have been several reports that CO oxidation occurs between adsorbed species in accordance with the Langmuir−Hinshelwood mechanism. By this mechanism, the first state of the reaction is considered to be the coadsorption of CO and O,[62,63] and to control the adsorption behavior and the activation energy for the reaction, the d-band center relative to the Fermi energy becomes a significant parameter.[64,65] As continuous control of the electronic structure of the PdRu solid-solution alloy with the metal composition was observed, it is considered that the d-band center in $Pd_{0.5}Ru_{0.5}$ becomes optimized for the absorption of O and CO and/or has a lower activation energy for the CO oxidation reaction.

We have also observed that PdRu solid-solution nanoparticles have a higher three-way catalytic activity than Rh

DOI: 10.1021/ar500413e
Acc. Chem. Res. 2015, 48, 1551−1559

nanoparticles.[66] From the viewpoint of the "elements strategy",[1] the 1:1 Pd−Ru solid-solution alloy acts as a more highly efficient catalyst than Rh, and the cost reduction results from the use of the cheaper elements Pd and Ru rather than Rh. Therefore, this work allowed us to create highly effective functional materials based on the novel strategy of interelement fusion.

5. CONCLUSION AND FUTURE PROSPECTS

This Account has focused on our recent efforts to establish "DOS engineering" for innovative functional materials based on the "interelement fusion" strategy. We have also demonstrated the development of synthetic methods for functional solid-solution alloy nanoparticles by approaches involving non-equilibrium synthesis or a process of hydrogen absorption/desorption. In the past two centuries, many methods have been developed to create alloys. In the future, the interelement fusion strategy will potentially be used to make full use of the 80 stable elements, allowing for the tuning of suitable DOS shapes for important catalytic applications such as fuel-cell electrocatalysis, exhaust gas purification, and steam -reforming of shale gas. Currently, the developments of these catalysts are mainly based on costly rare elements, and through the DOS engineering approach we hope to create higher-performance materials even while replacing or reducing minor or harmful elements through the combination of more abundant elements.

AUTHOR INFORMATION

Corresponding Author

*E-mail: kitagawa@kuchem.kyoto-u.ac.jp.

Notes

The authors declare no competing financial interest.

Biographies

Hirokazu Kobayashi received his Ph.D. from Kyushu University in 2008. He worked as a postdoctoral fellow at Washington University in St. Louis (2009) and as an assistant professor at the Institute for Integrated Cell-Material Sciences at Kyoto University (2009−2012). Since 2012 he has been an associate professor at the Graduate School of Science of Kyoto University. His research interests include the development of nanostructured hybrid materials for applications in catalysis and energy generation/storage. He created the PdPt solid-solution alloy nanoparticles.

Kohei Kusada received his Ph.D. in 2013 from Kyoto University under the supervision of Prof. Hiroshi Kitagawa. He worked as a JSPS Research Fellow (DC1) from 2010 to 2013. After a period at Asahi Kasei Chemicals Co. as a researcher (2013−2014), he moved back to Kyoto University as an assistant professor in Prof. Kitagawa's laboratory. He received the Springer Thesis Award for his thesis entitled "Creation of New Metal Nanoparticles and Their Hydrogen-Storage and Catalytic Properties." He created the AgRh and PdRu solid-solution alloy nanoparticles.

Hiroshi Kitagawa received his Ph.D. from Kyoto University in 1992. After working at the Institute for Molecular Science, the Japan Advanced Institute of Science and Technology, and the University of Tsukuba, he moved to Kyushu University as Professor of Inorganic Chemistry in 2003. In 2009 he returned to the laboratory at Kyoto University as Professor of Solid-State Chemistry. He held a visiting appointment at the Davy−Faraday Research Laboratory of the Royal Institution of Great Britain (1993−1994). He was Science Officer for the Ministry of Education, Culture, Sports, Science and Technology, Japan (2010−2014) and chair of the Fifth Chemical Sciences and Society Summit (CS3) in 2013. He is now Kyoto University's Assistant Executive Vice-President (Research) and a member of the Organizing Committee for Pacifichem 2015. He developed the chemistry of the solid-state properties of coordination compounds and nanomaterials. He has been awarded The Chemical Society of Japan Award for Creative Work (2010), the Inoue Prize for Science (2011), and the Premio Marco Polo della Scienza Italiana (2013).

REFERENCES

(1) Nakamura, E.; Sato, K. Managing the scarcity of chemical elements. *Nat. Mater.* **2011**, *10*, 158−161.
(2) Fukui, K. Role of Frontier Orbitals in Chemical Reactions. *Science* **1982**, *218*, 747−754.
(3) Kittel, C.; McEuen, P. *Introduction to Solid State Physics*; Wiley: New York, 1976.
(4) Fazekas, P. *Lecture Notes on Electron Correlation and Magnetism*; World Scientific: Singapore, 1999.
(5) Bianchini, C.; Shen, P. K. Palladium-Based Electrocatalysts for Alcohol Oxidation in Half Cells and in Direct Alcohol Fuel Cells. *Chem. Rev.* **2009**, *109*, 4183−4206.
(6) Centi, G. Supported Palladium Catalysts in Environmental Catalytic Technologies for Gaseous Emissions. *J. Mol. Catal. A: Chem.* **2001**, *173*, 287−312.
(7) Blaser, H.-U.; Indolese, A.; Schnyder, A.; Steiner, H.; Studer, M. Supported Palladium Catalysts for Fine Chemicals Synthesis. *J. Mol. Catal. A: Chem.* **2001**, *173*, 3−18.
(8) *Binary Alloy Phase Diagrams*; Massalski, T. B., Okamoto, H., Subramanian, P. R., Kacprzak, L., Eds.; ASM International: Materials Park, OH, 1990.
(9) Kubo, R. Electronic Properties of Metallic Fine Particles. I. *J. Phys. Soc. Jpn.* **1962**, *17*, 975−986.
(10) *Clusters and Colloids: From Theory to Applications*; Schmid, G., Ed.; VCH: Weinheim, Germany, 1994.
(11) Koga, K.; Ikeshoji, T.; Sugawara, K. Size- and Temperature-Dependent Structural Transitions in Gold nanoparticles. *Phys. Rev. Lett.* **2004**, *92*, No. 115504.
(12) Zhang, M.; Efremov, M. Y.; Schiettekatte, F.; Olson, E. A.; Kwan, A. T.; Lai, S. L.; Wisleder, T.; Greene, J. E.; Allen, H. Size-Dependent Melting Point Depression of Nanostructures: Nanocalorimetric Measurements. *Phys. Rev. B* **2000**, *62*, 10548−10564.
(13) Shibata, T.; Bunker, B. A.; Zhang, Z.; Meisel, D.; Vardeman, C. F.; Gezelter, J. D. Size-Dependent Spontaneous Alloying of Au−Ag Nanoparticles. *J. Am. Chem. Soc.* **2002**, *124*, 11989−11996.
(14) Yasuda, H.; Mori, H. Cluster-Size Dependence of Alloying Behavior in Gold Clusters. *Z. Phys. D* **1994**, *31*, 131−134.
(15) Kusada, K.; Kobayashi, H.; Yamamoto, T.; Matsumura, S.; Sumi, N.; Sato, K.; Nagaoka, K.; Kubota, Y.; Kitagawa, H. Discovery of the Face-Centered Cubic Ruthenium Nanoparticles: Facile Size-Controlled Synthesis using the Chemical Reduction Method. *J. Am. Chem. Soc.* **2013**, *135*, 5493−5496.
(16) Doyen, G.; Ertl, G. Theory of carbon monoxide chemisorption on transition metals. *Surf. Sci.* **1974**, *43*, 197−229.
(17) The band structures were calculated by T. Yayama, T. Ishimoto, and M. Koyama (Kyushu University).
(18) Greeley, J.; Nørskov, J. K.; Kibler, L. A.; El-Aziz, A. M.; Kolb, D. M. Hydrogen Evolution over Bimetallic Systems: Understanding the Trends. *ChemPhysChem* **2006**, *7*, 1032−1035.
(19) Nørskov, J. K.; Bligaard, T.; Rossmeisl, J.; Christensen, C. H. Towards the Computational Design of Solid Catalysts. *Nat. Chem.* **2009**, *1*, 37−46.
(20) Appleby, A. J. Electrocatalysis and fuel cells. *Catal. Rev.* **1970**, *4*, 221−243.
(21) Antolini, E. Catalysts for direct ethanol fuel cells. *J. Power Sources* **2007**, *170*, 1−12.
(22) Burch, R.; Breen, J. P.; Meunier, F. C. A review of the selective reduction of NO_x with hydrocarbons under lean-burn conditions with

DOI: 10.1021/ar500413e
Acc. Chem. Res. 2015, 48, 1551−1559

non-zeolitic oxide and platinum group metal catalysts. *Appl. Catal., B* **2002**, *39*, 283−303.
(23) Yang, J.; Lee, J. Y.; Zhang, Q.; Zhou, W.; Liu, Z. Carbon-Supported Pseudo-Core−Shell Pd−Pt Nanoparticles for ORR with and without Methanol. *J. Electrochem. Soc.* **2008**, *155*, B776−B781.
(24) Toshima, N.; Shiraishi, Y.; Shiotsuki, A.; Ikenaga, D.; Wang, Y. Novel Synthesis Structure and Catalysis of Inverted Core/Shell Structured Pd/Pt Bimetallic Nanoclusters. *Eur. Phys. J. D* **2001**, *16*, 209−212.
(25) Lim, B.; Jiang, M.; Camargo, P. H. C.; Cho, E. C.; Tao, J.; Lu, X.; Zhu, Y.; Xia, Y. Pd−Pt Bimetallic Nanodendrites with High Activity for Oxygen Reduction. *Science* **2009**, *324*, 1302−1305.
(26) Lim, B.; Wang, J.; Camargo, P. H.; Cobley, C. M.; Kim, M. J.; Xia, Y. Twin-Induced Growth of Palladium−Platinum Alloy Nanocrystals. *Angew. Chem., Int. Ed.* **2009**, *48*, 6304−6308.
(27) Bharadwaj, S. R.; Kerkar, A. S.; Tripathi, S. N.; Dharwadkar, S. R. The Palladium−Platinum Phase Diagram. *J. Less-Common Met.* **1991**, *169*, 167−172.
(28) Kobayashi, H.; Yamauchi, M.; Kitagawa, H.; Kubota, Y.; Kato, K.; Takata, M. Atomic-Level Pd−Pt Alloying and Largely Enhanced Hydrogen-Storage Capacity in Bimetallic Nanoparticles Reconstructed from Core/Shell Structure by a Process of Hydrogen Absorption/Desorption. *J. Am. Chem. Soc.* **2010**, *132*, 5576−5577.
(29) Kobayashi, H.; Yamauchi, M.; Kitagawa, H.; Kubota, Y.; Kato, K.; Takata, M. Hydrogen Absorption in the Core/Shell Interface of Pd/Pt Nanoparticles. *J. Am. Chem. Soc.* **2008**, *130*, 1818−1819.
(30) Yamauchi, M.; Ikeda, R.; Kitagawa, H.; Takata, M. Nanosize Effects on Hydrogen Storage in Palladium. *J. Phys. Chem. C* **2008**, *112*, 3294−3299.
(31) Kobayashi, H.; Yamauchi, M.; Kitagawa, H.; Kubota, Y.; Kato, K.; Takata, M. On the Nature of Strong Hydrogen Atom Trapping inside Pd Nanoparticles. *J. Am. Chem. Soc.* **2008**, *130*, 1828−1829.
(32) Yamauchi, M.; Kobayashi, H.; Kitagawa, H. Hydrogen Storage Mediated by Pd and Pt Nanoparticles. *ChemPhysChem* **2009**, *10*, 2566−2576.
(33) Kobayashi, H.; Yamauchi, M.; Ikeda, R.; Kitagawa, H. Atomic-Level Pd−Au Alloying and Controllable Hydrogen-Absorption Properties in Size-Controlled Nanoparticles Synthesized by Hydrogen Reduction Method. *Chem. Commun.* **2009**, 4806−4808.
(34) Kobayashi, H.; Morita, H.; Yamauchi, M.; Kitagawa, H.; Kubota, Y.; Kato, K.; Takata, M. Nanosize-Induced Hydrogen Storage and Capacity Control in a Non-Hydride-Forming Element: Rhodium. *J. Am. Chem. Soc.* **2011**, *133*, 11034−11037.
(35) Kobayashi, H.; Yamauchi, M.; Kitagawa, H. Finding Hydrogen-Storage Capability in Iridium Induced by the Nanosize Effect. *J. Am. Chem. Soc.* **2012**, *134*, 6893−6895.
(36) Kobayashi, H.; Morita, H.; Yamauchi, M.; Kitagawa, H.; Kubota, Y.; Kato, K.; Takata, M. Nanosize-Induced Drastic Drop in Equilibrium Hydrogen Pressure for Hydride Formation and Structural Stabilization in Pd−Rh Solid-Solution Alloys. *J. Am. Chem. Soc.* **2012**, *134*, 12390−12393.
(37) *Hydrogen in Metals*; Alefeld, G., Völkl, J., Eds.; Springer: Berlin, 1978.
(38) Bowker, M. Automotive Catalysis Studied by Surface Science. *Chem. Soc. Rev.* **2008**, *37*, 2204−2211.
(39) Inderwildi, O. R.; Jenkins, S. J.; King, D. A. Dynamic Interplay between Diffusion and Reaction: Nitrogen Recombination on Rh{211} in Car Exhaust Catalysis. *J. Am. Chem. Soc.* **2008**, *130*, 2213−2220.
(40) Guo, J.; Hsu, A.; Chu, D.; Chen, R. Improving Oxygen Reduction Reaction Activities on Carbon-Supported Ag Nanoparticles in Alkaline Solutions. *J. Phys. Chem. C* **2010**, *114*, 4324−4330.
(41) Gera, V. B.; Gupta, R.; Jain, K. P. Electronic Structure of III−V Ternary Semiconductors. *J. Phys.: Condens. Matter* **1989**, *1*, 4913−4930.
(42) Papaconstantopoulos, D. A.; Klein, B. M.; Economou, E. N.; Boyer, L. L Band Structure and Superconductivity of PdD_x and PdH_x. *Phys. Rev. B* **1978**, *17*, 141−150.
(43) Wicke, E. Electronic Structure and Properties of Hydrides of 3d and 4d Metals and Intermetallics. *J. Less-Common Met.* **1984**, *101*, 17−33.
(44) Karakaya, I.; Thompson, W. T. The Ag−Rh (Silver−Rhodium) System. *Bull. Alloy Phase Diagrams* **1986**, *7*, 362−365.
(45) Kusada, K.; Yamauchi, M.; Kobayashi, H.; Kitagawa, H.; Kubota, Y. Hydrogen-Storage Properties of Solid-Solution Alloys of Immiscible Neighboring Elements with Pd. *J. Am. Chem. Soc.* **2010**, *132*, 15896−15898.
(46) Yang, A.; Sakata, O.; Kusada, K.; Yayama, T.; Yoshikawa, H.; Ishimoto, T.; Koyama, M.; Kobayashi, H.; Kitagawa, H. The valence band structure of Ag_xRh_{1-x} alloy nanoparticles. *Appl. Phys. Lett.* **2014**, *105*, No. 153109.
(47) Tripathi, S. N.; Bharadwaj, S. R.; Dharwadkar, S. R. The Pd−Ru System (Palladium−Ruthenium). *J. Phase Equilib.* **1993**, *14*, 638−642.
(48) Perkas, N.; Teo, J.; Shen, S.; Wang, Z.; Highfield, J.; Zhong, Z.; Gedanken, A. Supported Ru Catalysts Prepared by Two Sonication-Assisted Methods for Preferential Oxidation of CO in H_2. *Phys. Chem. Chem. Phys.* **2011**, *13*, 15690−15698.
(49) Hecker, W. C.; Bell, A. T. Reduction of NO by CO over Silica-Supported Rhodium: Infrared and Kinetic Studies. *J. Catal.* **1983**, *84*, 200−215.
(50) Grass, M. E.; Zhang, Y.; Butcher, D. R.; Park, J. Y.; Li, Y.; Bluhm, H.; Bratlie, K. M.; Zhang, T.; Somorjai, G. A. A Reactive Oxide Overlayer on Rhodium Nanoparticles during CO Oxidation and Its Size Dependence Studied by in Situ Ambient-Pressure X-ray Photoelectron Spectroscopy. *Angew. Chem., Int. Ed.* **2008**, *47*, 8893−8896.
(51) Joo, S. H.; Park, J. K.; Renzas, J. R.; Butcher, D. R.; Huang, W.; Somorjai, G. A. Size Effect of Ruthenium Nanoparticles in Catalytic Carbon Monoxide Oxidation. *Nano Lett.* **2010**, *10*, 2709−2713.
(52) Ertl, G. Reactions at Surfaces: From Atoms to Complexity (Nobel Lecture). *Angew. Chem., Int. Ed.* **2008**, *47*, 3524−3535.
(53) Xiao, L.; Zhuang, L.; Liu, Y.; Lu, J.; Abruna, H. D. Activating Pd by Morphology Tailoring for Oxygen Reduction. *J. Am. Chem. Soc.* **2009**, *131*, 602−608.
(54) Newton, M. A.; Belver-Coldeira, C.; Martínez-Arias, A.; Fernández-García, M. Dynamic in Situ Observation of Rapid Size and Shape Change of Supported Pd Nanoparticles during CO/NO Cycling. *Nat. Mater.* **2007**, *6*, 528−532.
(55) Schultz, N. E.; Gherman, B. E.; Cramer, C. J.; Truhlar, D. G. Pd_nCO (n = 1, 2): Accurate Ab Initio Bond Energies, Geometries, and Dipole Moments and the Applicability of Density Functional Theory for Fuel Cell Modeling. *J. Phys. Chem. B* **2006**, *110*, 24030−24046.
(56) Lee, H. C.; Potapova, Y.; Lee, D. A core−shell structured, metal−ceramic composite-supported Ru catalyst for methane steam reforming. *J. Power Sources* **2012**, *216*, 256−260.
(57) McFarland, E. Unconventional Chemistry for Unconventional Natural Gas. *Science* **2012**, *338*, 340−342.
(58) Abdelsayed, V.; Aljarash, A.; El-Shall, M. S.; Othman, Z. A. A.; Alghamdi, A. H. Microwave Synthesis of Bimetallic Nanoalloys and CO Oxidation on Ceria-Supported Nanoalloys. *Chem. Mater.* **2009**, *21*, 2825−2834.
(59) Renzas, J. R.; Huang, W.; Zhang, Y.; Grass, M. E.; Hoang, D. T.; Alayoglu, S.; Butcher, D. R.; Tao, F.; Liu, Z.; Somorjai, G. A. $Rh_{1-x}Pd_x$ nanoparticle composition dependence in CO oxidation by oxygen: Catalytic activity enhancement in bimetallic systems. *Phys. Chem. Chem. Phys.* **2011**, *13*, 2556−2562.
(60) Kusada, K.; Kobayashi, H.; Ikeda, R.; Kubota, Y.; Takata, M.; Toh, S.; Yamamoto, T.; Matsumura, S.; Sumi, N.; Sato, K.; Nagaoka, K.; Kitagawa, H. Solid Solution Alloy Nanoparticles of Immiscible Pd and Ru Elements Neighboring on Rh: Changeover of the Thermodynamic Behavior for Hydrogen Storage and Enhanced CO-Oxidizing Ability. *J. Am. Chem. Soc.* **2014**, *136*, 1864−1871.
(61) Qadir, K.; Joo, S. H.; Mun, B. S.; Butcher, D. R.; Renzas, J. R.; Aksoy, F.; Liu, Z.; Somorjai, G. A.; Park, J. Y. Intrinsic Relation between Catalytic Activity of CO Oxidation on Ru Nanoparticles and Ru Oxides Uncovered with Ambient Pressure XPS. *Nano Lett.* **2012**, *12*, 5761−5768.

DOI: 10.1021/ar500413e
Acc. Chem. Res. 2015, 48, 1551−1559

(62) Engel, T.; Ertl, G. A Molecular Beam Investigation of the Catalytic Oxidation of CO on Pd(111). *J. Chem. Phys.* **1978**, *69*, 1267−1281.
(63) Liu, K.; Wang, A.; Zhang, T. Recent Advances in Preferential Oxidation of CO Reaction over Platinum Group Metal Catalysts. *ACS Catal.* **2012**, *2*, 1165−1178.
(64) Hammer, B.; Nørskov, J. K. Why Gold is the Noblest of All the Metals. *Nature* **1995**, *376*, 238−240.
(65) Hammer, B.; Nørskov, J. K. Electronic Factors Determining the Reactivity of Metal Surfaces. *Surf. Sci.* **1995**, *343*, 211−220.
(66) Sato, K.; Tomonaga, H.; Yamamoto, T.; Matsumura, S.; Kusada, K.; Kobayashi, H.; Kitagawa, H.; Nagaoka, K. To be submitted.

DOI: 10.1021/ar500413e
Acc. Chem. Res. 2015, 48, 1551−1559